Cell Metabolism
Article

Histone Demethylase UTX-1 Regulates *C. elegans* Life Span by Targeting the Insulin/IGF-1 Signaling Pathway

Chunyu Jin,[1,3,4,8] Jing Li,[1,3,4,8] Christopher D. Green,[1,8] Xiaoming Yu,[1,3,4] Xia Tang,[1] Dali Han,[1,3,4] Bo Xian,[1,3,4] Dan Wang,[1,3,4] Xinxin Huang,[5] Xiongwen Cao,[2] Zheng Yan,[1] Lei Hou,[1,3,4] Jiancheng Liu,[1,3,4] Nicholas Shukeir,[6] Philipp Khaitovich,[1,7] Charlie D. Chen,[2] Hong Zhang,[5] Thomas Jenuwein,[6] and Jing-Dong J. Han[1,*]
[1]Chinese Academy of Sciences Key Laboratory of Computational Biology, Chinese Academy of Sciences-Max Planck Partner Institute for Computational Biology
[2]Institute of Biochemistry and Cell Biology
Shanghai Institutes for Biological Sciences, Chinese Academy of Sciences, 320 Yue Yang Road, Shanghai, 200031, China
[3]Center for Molecular Systems Biology, Institute of Genetics and Developmental Biology, Chinese Academy of Sciences, Datun Road, Beijing, 100101, China
[4]Graduate University of Chinese Academy of Sciences, Yuquan Road, Beijing, 100049, China
[5]National Institute of Biological Sciences, Zhongguancun Science Park, Beijing, 102206, China
[6]Max Planck Institute for Immunobiology and Epigenetics, Stubeweg 51, D-79108, Freiberg, Germany
[7]Max Planck Institute for Evolutionary Anthropology, Deutscher Platz 6, Leipzig, Germany
[8]These authors contributed equally to this work
*Correspondence: jdhan@picb.ac.cn
DOI 10.1016/j.cmet.2011.07.001

SUMMARY

Epigenetic modifications are thought to be important for gene expression changes during development and aging. However, besides the Sir2 histone deacetylase in somatic tissues and H3K4 trimethylation in germlines, there is scant evidence implicating epigenetic regulations in aging. The insulin/IGF-1 signaling (IIS) pathway is a major life span regulatory pathway. Here, we show that progressive increases in gene expression and loss of H3K27me3 on IIS components are due, at least in part, to increased activity of the H3K27 demethylase UTX-1 during aging. RNAi of the *utx-1* gene extended the mean life span of *C. elegans* by ~30%, dependent on DAF-16 activity and not additive in *daf-2* mutants. The loss of *utx-1* increased H3K27me3 on the *Igf1r/daf-2* gene and decreased IIS activity, leading to a more "naive" epigenetic state. Like stem cell reprogramming, our results suggest that reestablishment of epigenetic marks lost during aging might help "reset" the developmental age of animal cells.

INTRODUCTION

Aging is a general and complex biological process that predisposes humans to many complex diseases, including neural degenerative diseases, type 2 diabetes, cardiovascular diseases, and various cancers (Campisi, 2005; Chien and Karsenty, 2005; Harman, 2006; Kirkwood, 2005; Longo and Kennedy, 2006). Genetic screens and naturally occurring mutations have identified hundreds of genes that affect aging and/or longevity. Among the many genes that affect organismal life span, the insulin/IGF-1 signaling (IIS) pathway stands out as a highly conserved and critical pathway among all organisms studied, regulating both organism development and aging (Antebi, 2007; Kenyon, 2005).

In *C. elegans*, the IIS pathway starts from an insulin-like receptor DAF-2 (Kimura et al., 1997). When activated by the insulin-like ligands, it recruits a PI3 kinase (AGE-1/AAP-1) (Morris et al., 1996) and then induces phosphorylation of the downstream serine/threonine kinases AKT-1, AKT-2, SGK-1, and PDK-1 (Hertweck et al., 2004; Paradis et al., 1999; Paradis and Ruvkun, 1998). This cascade in turn phosphorylates the forkhead transcription factor (FOXO), DAF-16 (Lin et al., 1997; Ogg et al., 1997), and prevents it from entering the nucleus to activate antiaging genes, such as genes that confer resistance to heat, oxidative stress and DNA damage (Hsu et al., 2003; Jia et al., 2004; Lamitina and Strange, 2005; Libina et al., 2003; Murakami and Johnson, 1996; Murphy et al., 2003).

Epigenetic modifications play important roles in transcriptional regulation (Berger, 2007; Klose and Zhang, 2007; Li et al., 2007; Wu and Zhang, 2009; Yu et al., 2008) and in organism development (Brosch et al., 2008; Jiang et al., 2008; Weishaupt et al., 2010). Similar to development, changes in gene expression and cellular activity status during aging are subject to modulation by epigenetic modifications, as an organism essentially has the same genomic sequences in young and old ages. However, other than the NAD-dependent histone deacetylase Sir2 and its mammalian homolog SIRT1 gene's regulation on longevity (Dang et al., 2009; Guarente and Picard, 2005; Oberdoerffer et al., 2008) and the recent finding of high levels of germline histone H3 lysine 4 trimethylation (H3K4me3) being detrimental to *C. elegans* life span (Greer et al., 2010), there is scant evidence demonstrating causality of epigenetic regulations on aging. The premature aging disease Hutchinson-Gilford Progeria Syndrome (HGPS) has been reported to be associated with loss of histone H3 trimethylation on lysine 27 (H3K27me3). In cells from a female HGPS patient, H3K27me3, a mark for gene inactivation, is lost

on the inactive X chromosome (Xi). The methyltransferase responsible for generating this mark, EZH2, is also downregulated (Shumaker et al., 2006). The level of histone methylations is controlled by the balance between histone methyltransferase and demethylase activities (Martin and Zhang, 2005; Shi, 2007). In mammals, two genes UTX/KDM6A and JMJD3/KDM6B have been identified as demethylases for H3K27me3 (Agger et al., 2007; Hong et al., 2007). By removing the transcriptionally repressive H3K27me3 mark, UTX and JMJD3 can antagonize transcriptional repression exerted by Polycomb repressor complexes, which are critical regulators of development in response to external or internal cues (De Santa et al., 2007; Lee et al., 2007; Swigut and Wysocka, 2007).

The *C. elegans* UTX-1 contains tetratricopeptide repeats (Tpr) and JmjC domains and is orthologous to the mammalian UTX (Swigut and Wysocka, 2007). There are three other UTX-1 paralogs in *C. elegans* F18E9.5, C29F7.6, and F23D12.5, which all contain only a JmjC domain, but no Tpr domain, indicating that they are more related to human JMJD3 than to UTX.

In spite of the rapid progress in finding molecular interactions for UTX, the discovery of its biological function is just beginning. The zebrafish *utx* gene has been shown to be required for posterior development in zebrafish through targeting the *Hox* genes (Lan et al., 2007). At the cellular level, UTX is involved in RB-dependent cell-cycle control (Wang et al., 2010). In *C. elegans*, no biological functions have been described for *utx-1*, although a mutation in an *utx-1* paralog *F18E9.5*, a *C. elegans* ortholog of the human *JMJD3* gene, has been shown to result in abnormal gonad development (Agger et al., 2007).

Here, we show that the *C. elegans utx-1* gene is an aging regulator by modulating the epigenetic and expression status of the IIS pathway genes. RNA interference (RNAi) of the *utx-1* gene extended the mean life span of *C. elegans* by ~30%. This effect was dependent on the DAF-16 activity. The longer-than-normal life span of *daf-2* mutants cannot be further extended by *utx-1* RNAi. The *daf-2/Igf1r* gene and its downstream genes were all downregulated by *utx-1* RNAi, resulting in increased nuclear accumulation of DAF-16. We observed a sharp increase of *utx-1* expression during aging, which preceded the increase in *daf-2* expression and mortality rate. We further show that *utx-1* RNAi significantly increased the H3K27me3 modification on the *daf-2* gene and that H3K27me3 on *daf-2* is significantly reduced in aged versus young worms. Similar age-dependent changes were also observed in rhesus macaque muscles and brain samples. Our findings suggest that downregulation of UTX-1 keeps the IIS pathway at a "younger" epigenetic state with high H3K27me3 modifications to delay the normal aging process, an aging regulatory mechanism that might be conserved from invertebrate to mammals.

RESULTS

Gene Expression of *utx-1* Changes during Aging

Given the hints from H3K27me3 changes in the progeria disease HGPS, we examined whether the expression levels of the H3K27me3 methyltransferase and demethylases change during normal aging using published human brain gene expression profiles measured by microarrays (Lu et al., 2004). The H3K27me3 methyltransferase *EZH2* displayed a marginally significant decrease (Student's t test, $p = 0.101$ or 0.044 with or without outliers), while the H3K27me3 demethylase *JMJD3* display no significant age-dependent expression changes ($p = 0.375$ or 0.22 for *JMJD3* with or without outliers). In contrast, the expression level of the other H3K27me3 demethylase *UTX* increases significantly in old age (Figure 1A and Figure S1 available online, $p = 0.004$ or 0.00011 with or without outliers).

We then confirmed the age-dependent change of the *utx-1* gene in *C. elegans* by real-time quantitative PCR (qPCR). The expression of *utx-1* showed a clear bimodal pattern. During young adulthood (day 0 to day 5), the *utx-1* expression level was very low, then after day 7 of adulthood the level dramatically increased, and steadily increased to a higher level by day 15 (Figure 1B). Interestingly, the sharp increase of the *utx-1* expression level immediately precedes the beginning of the increase in mortality (Figures 1B and 1C). In comparison, the other *utx-1* paralogs, F18E9.5, C29F7.6, and F23D12.5, did not show persistent expression increase in aging worms (Figure 1B). We therefore hypothesized that downregulating the UTX-1 activity might delay the aging process.

Downregulation of *utx-1* Increased Life Span in *C. elegans*

When worms were fed from L1 and onward bacteria containing double-stranded RNA (dsRNA) against *utx-1* or an empty dsRNA vector as control, the *utx-1* RNAi extended the mean life span by ~30% compared to worms fed with vector RNAi bacteria (Figure 1C and Table S1). Meanwhile, there was no significant abnormal phenotype in development, including maturation time, egg laying, body length, and male tail development (data not shown), which indicates that the life span extension was mainly caused by delaying aging rather than development abnormalities. To rule out off-target effects, although there is little such possibility given that long dsRNA sequences are required for effectively knocking down gene activity in *C. elegans*, we first confirmed that the RNAi specifically targeted *utx-1* instead of its paralogs (Figure S1C), then we also generated another RNAi construct targeting a region of *utx-1* that is nonoverlapping with the first construct and obtained similar results in a life span assay (Figure 1C, RNAi #2). This second RNAi construct did not knock down the *utx-1* gene as much as the original RNAi construct from the Ahringher library (Figure 1C, right panel); it is therefore not surprising that its life span extension was not as much as with RNAi #1 (Figure 1C). RNAi of an H3K4 methyltansferase complex gene *ash-2* has been found to increase life span under no-FUdR conditions (Greer et al., 2010). Under such conditions, the life span extensions in wild-type N2 worms by *utx-1* RNAi is comparable to that by *ash-2* RNAi (Figure 1D and Table S1). To further confirm this result, we also examined the life span of a heterozygous *utx-1* deletion mutant. Because *utx-1* homozygous mutant is lethal, we generated *utx-1* heterozygote *tm3118*/+ balanced by AF1 (+/*szT1[lon-2(e678)]* I; *dpy-8(e1321) unc-3(e151)/szT1* X). Consistent with the life span extension by *utx-1* RNAi, *utx-1* heterozygote *tm3118*/+ also displayed increased mean and maximum life span compared to its parental AF1 strain (Figure 1E). Another *utx-1* heterozygous mutant *ok3553* also displayed significant life span extension compared with its parental strain (Figure 1E and Table S2).

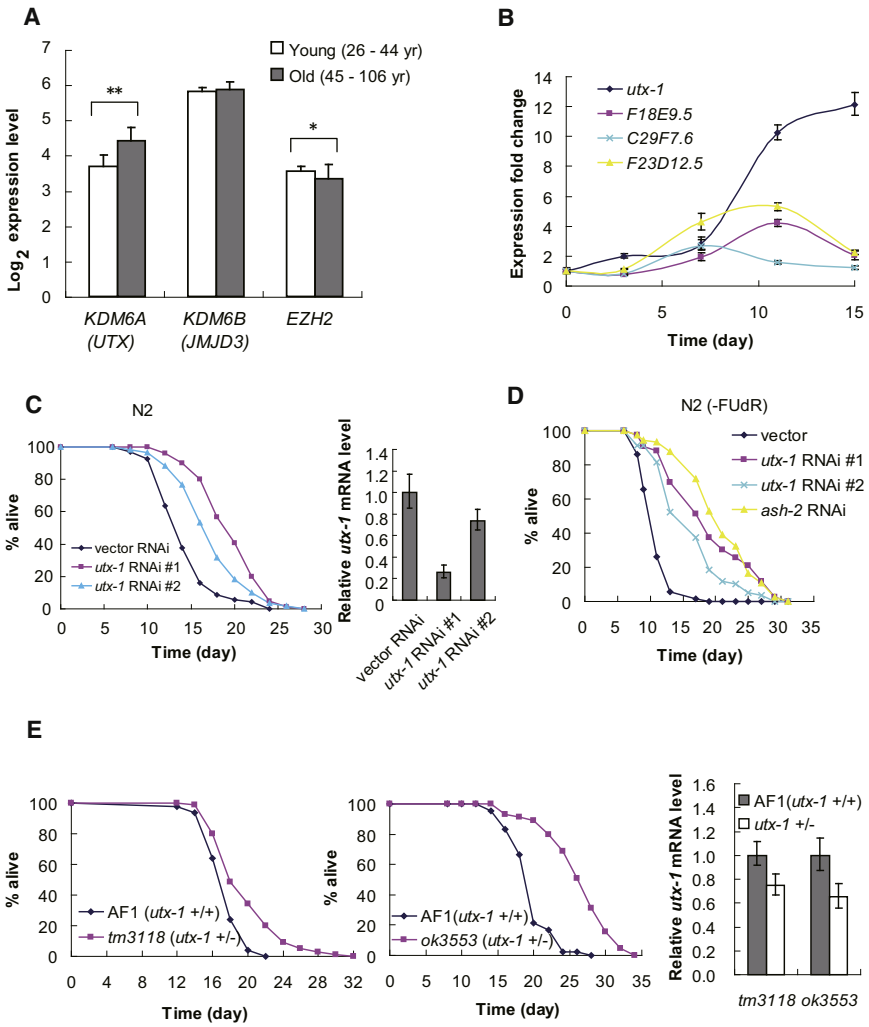

Figure 1. UTX-1 Regulates *C. elegans* Life Span

(A) Average expression levels of *EZH2*, *JMJD3*, and *UTX* in the young and old human brains. Expression values were extracted from a microarray data set. The young group contains ten samples from ages 26 to 44 years, and the old group contains 20 samples from 45 to 106 years according to the observations in Lu et al. (2004). Use of different groupings identified by unsupervised hierarchical clustering gives similar results (Figure S1). An error bar of a group indicates the standard deviation (SD) within the group. ** indicates Student's t test $p < 0.01$, while * indicates $p < 0.05$.

(B) The expression levels of *utx-1* and its three paralogs, F18E9.5, C29F7.6, and F23D12.5, during *C. elegans* aging. Real-time qPCR quantification of *utx-1* cDNA was done at day 0, 3, 7, 11, and 15 of adulthood. Error bars represent the SD of three independent replicates. β-actin mRNA level was used as an internal control.

(C) *utx-1* RNAi increased life span in wild-type N2 worms. Bacteria containing RNAi #1 construct was picked from the Ahrigher RNAi library; #2 was constructed by us, and shares no overlap with #1. Their RNAi efficiencies were determined by qPCR and shown in the right panel. Error bars indicate the standard error of mean (SEM) of three repeats. β-actin mRNA level was used as an internal control. The mean life span and SD are listed in Table S1.

(D) Life span curves of *utx-1* or *ash-2* RNAi in N2 worms without FUdR. The mean life span and SD are listed in Table S1.

(E) *utx-1* heterozygote *tm3118*/+ or *ok3553*/+ had extended life span compared to its parental strain AF1. Log-rank test, p = 1.13E-05 and 3.59E-12, respectively. Insets show relative expression level of *utx-1* in *utx-1* heterozygote *tm3118*/+ or *ok3553*/+ compared with its balancer strain AF1 as quantified by qPCR. Error bars indicate the SEM of three repeats. β-actin mRNA level was used as an internal control. Statistics are presented in Table S2.

See also Figure S1 and Tables S1–S3.

In *C. elegans*, there are three other genes homologous to UTX-1 that may also be responsible for H3K27me3 demethylation, F18E9.5, C29F7.6, and F23D12.5, all of which are orthologous to the human JMJD3 rather than UTX protein. We asked whether these UTX-1 paralogs have the same effect on life span. *C29F7.6* and *F23D12.5* RNAi also slightly extended life span, but not as strong as *utx-1(D2021.1)* RNAi (Figure S1D and Table S3). On the contrary, *F18E9.5* (the best match to human *JMJD3*) RNAi shortened life span in N2 worms, which might be related to its requirement in gonadal development (Agger et al., 2007). These results indicate that H3K27me3 indeed might be a regulatory event for aging; however, the differential effect of different H3K27me3 demethylases implicates that their target genes are at least partially different (Swigut and Wysocka, 2007).

UTX-1 Is Involved in Heat, UV, and Oxidative Stress Response Regulation

Increased longevity has been known to correlate with tolerance to multiple stresses, such as heat, ultraviolet (UV) light and oxidative stresses (Hsu et al., 2003; Lee et al., 2003; Murphy et al., 2003). We therefore tested whether *utx-1* knockdown worms are more resistant to these stresses. Compared to worms fed with empty vector RNAi bacteria, *utx-1* RNAi did make worms more resistant to 35°C heat shock, UV, and paraquat treatments, which represent heat, DNA damage, and oxidative stresses, respectively (Figure 2 and Table S4). Similar increases in heat and UV stress resistance were also observed for *utx-1* heterozygote *tm3118*/+ (Figure S2A and Table S4). These demonstrate that lowered *utx-1* expression resulted in higher stress resistance. In addition, since these stress resistances are tightly coupled to life span regulation through the IIS pathway (Dillin et al., 2002; Finkel and Holbrook, 2000; Lithgow et al., 1995; Murakami and Johnson, 1996), this result also implicates that *utx-1* might regulate aging through the IIS pathway. We also confirmed that the life span extension induced by *utx-1* RNAi was not caused by affecting amphid neurons (Figure S2B). Out of 45 control and 50 *utx-1* RNAi worms examined, none of them had any defects in amphid neurons or the *Dyf* phenotype.

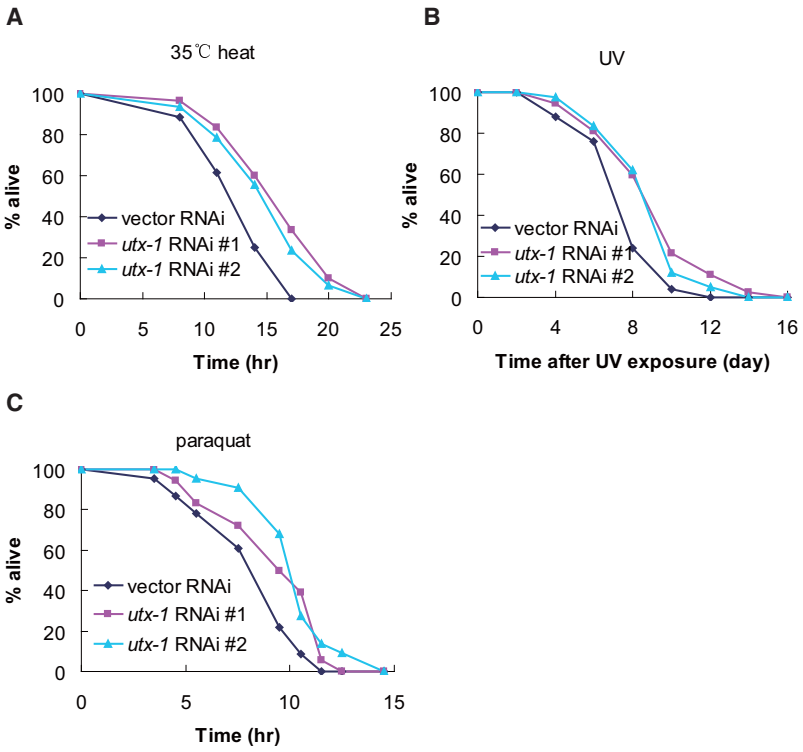

Figure 2. Reduced *utx-1* Level Enhanced *C. elegans* Resistance to Heat, UV, and Oxidative Stresses

Survival curves of wild-type N2 worms fed bacteria containing dsRNA of *utx-1* or empty vector from L1 stage and onward subjected to heat (A), DNA damage (B), or oxidative stress (C). For heat treatment, animals were shifted to 35°C on day 3 of adulthood (log-rank test on the Kaplan-Meier curves, p = 6.86E-05 and 2.8E-04 for *utx-1* RNAi #1 and #2, respectively). For DNA damage treatment, animals were exposed to 1200J/m^2 UV on day 3 of adulthood (p = 0.00106 and 0.00235 for *utx-1* RNAi #1 and #2). For oxidative stress treatment, animals were dipped into 100 mM paraquat on day 3 of adulthood (p = 0.05 and 0.002 for *utx-1* RNAi #1 and #2). See also Figure S2 and Table S4.

Life Span Extension by *utx-1* RNAi Is Dependent on *daf-16* Activity and IIS Pathway

Both longevity and stress tolerance are known to be promoted by the forkhead transcription factor DAF-16 and suppressed by its upstream IIS pathway genes, such as the insulin-like growth factor receptor *daf-2*. The *daf-2(e1370)* mutant worms have an extended life span, while *daf-16(mu86)* mutant animals have a very short life span. To investigate the functional connection between *utx-1* and genes in the IIS pathway, we examined the life span changes upon knockdown of *utx-1* in *daf-2(e1370)* and *daf-16(mu86)* mutants. While *utx-1* RNAi effectively extended the life span of wild-type N2 strain, such an effect could not be observed in any mutant on IIS pathway (Figures 3A–3F and Table S5); *utx-1* RNAi could not further increase the life span of *daf-2(e1370)* worms (Figure 3A) and could not at all increase the life span in *daf-16(mu86)* mutant animals (Figure 3B). These results indicate that the *utx-1* RNAi-induced longevity is dependent on *daf-16* activity and that *utx-1* acts in the same pathway as *daf-2*. Further confirming that *utx-1* functions in this pathway, the life span extension by *utx-1* RNAi was also abolished in three other mutants *akt-1(ok525)*, *akt-2(ok393)*, *sgk-1(ok538)*, which are defective in the IIS pathway (Figures 3C–3E).

As *daf-2* RNAi extends life span in a germline-independent manner (Arantes-Oliveira et al., 2003), we tested whether *utx-1* directly acts in the soma as opposed to the germline by selectively knocking down *utx-1* in germ cells in *rrf-1(ok589)* mutant, where RNAi does not work in somatic cells but works effectively in germ cells. RNAi of *utx-1* could not extend the life span of *rrf-1(ok589)* worms, while *ash-2* RNAi could (Figure 3G). In contrast, *utx-1* RNAi can still further extend life span of the germline lacking *glp-1(e2141)* mutant (Figure 3H). These results indicate UTX-1's modulation of life span is independent of the germline, but instead acts directly in the soma.

To further verify the connection between *utx-1* and the IIS pathway by other phenotypes, we compared the stress resistance of *daf-16(mu86)* mutant worms upon *utx-1* RNAi with the same strain treated with empty vector. Consistent with the requirement of *daf-16* for *utx-1* RNAi-induced life span extension, no survival rate difference between *utx-1* and vector RNAi in *daf-16(mu86)* worms was observed under heat, UV, or paraquat treatment (Figure S2C and Table S4), indicating that *daf-16* is also required for *utx-1* RNAi induced stress resistances. Together, these results demonstrate that *utx-1* regulates life span and stress tolerance through the IIS pathway.

DAF-2 expresses mainly in intestine, nervous system and head neurons (McKay et al., 2003). We therefore examined whether UTX-1 also expresses in these tissues by using a GFP construct driven by the *utx-1* promoter (P*utx-1*::*gfp*). Broad expression in tissues including the IIS targeting tissues was found for this reporter (Figure 4A). Moreover, we examined the colocalization of *utx-1* and *daf-2* in a strain coexpressing P*utx-1*::*gfp* and *daf-2* promoter-driven mCherry (P*daf-2*::*mCherry*), which represents the DAF-2 expression patterns. As expected, the expression pattern of these two genes merged well, especially in the intestine (Figure 4B). The colocalization of *daf-2* and *utx-1* gene expression is consistent with its functional interaction with the IIS pathway.

UTX-1 Regulates IIS Gene Expression

As UTX-1 is a putative H3K27me3 demethylase that can remove this repressive epigenetic mark and activate gene expression, we asked whether UTX-1 regulates the gene expression of the IIS pathway genes. We performed qPCR to detect the expression level of IIS genes in wild-type N2 worms treated with *utx-1* or empty vector RNAi, using a housekeeping gene β-actin as an internal control. The transcript levels of *daf-2, age-1, akt-1*, *akt-2*, and *sgk-1,* all of which are upstream of *daf-16* and negatively regulate DAF-16 nuclear translocation, were all decreased in *utx-1* RNAi animals compared with vector RNAi (Figure 5A, primers in Table S7). A similar direction of

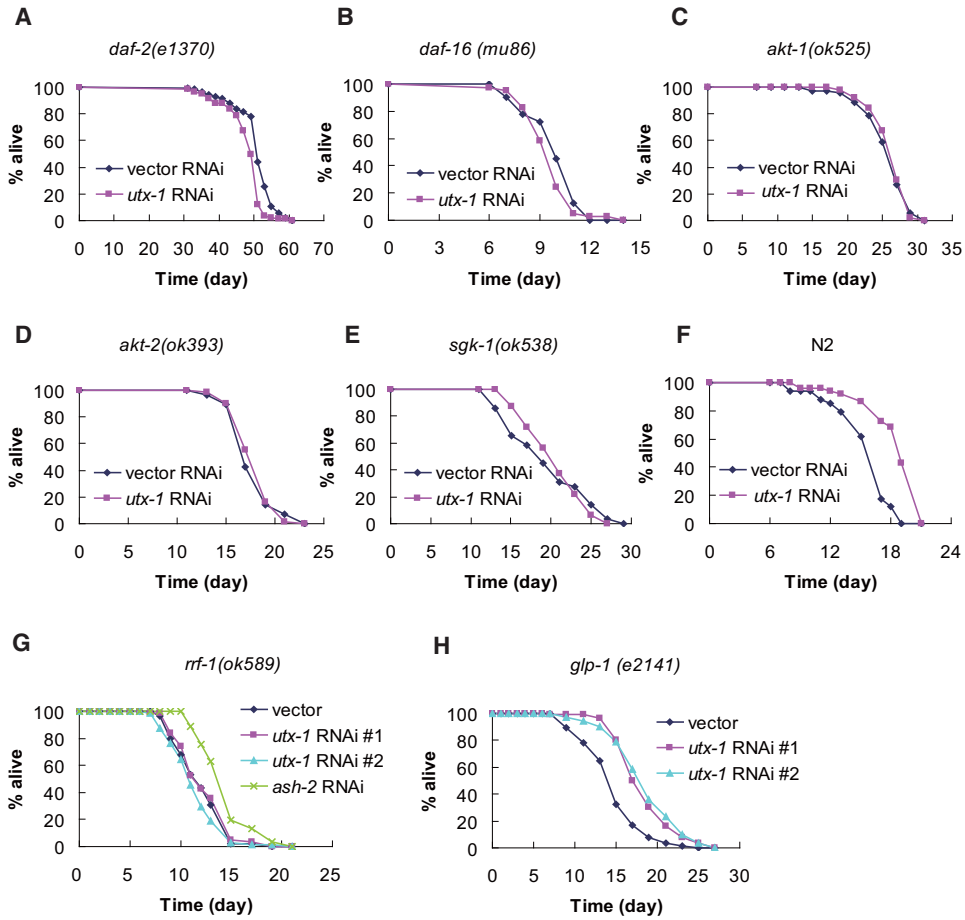

Figure 3. Longevity Regulation by *utx-1* Is Dependent on *daf-16* Activity and Acts through the IIS Pathway

(A–F) Survival curves of IIS pathway mutant *daf-2(e1370)* (A), *daf-16(mu86)* (B), *akt-1(ok525)* (C), *akt-2 (ok393)* (D), *sgk-1(ok538)* (E), and wild-type N2 worms (F), with vector or *utx-1* RNAi. The mean life span of *daf-2(e1370)* with *utx-1* RNAi was not longer, but shorter than that with vector RNAi (p = 1.22E-07). The mean life span *daf-16(mu86)* with *utx-1* RNAi was indistinguishable from that of vector RNAi, p = 0.59; so are *akt-1(ok525)* with *utx-1* RNAi versus with vector RNAi p = 0.65; *akt-2(ok393)* with *utx-1* RNAi versus with vector RNAi, p = 0.73; *sgk-1(ok538)* with *utx-1* RNAi versus vector RNAi, p = 0.67. Statistics are presented in Table S5.

(G) Life span extension by *utx-1* RNAi is abolished in *rrf-1(ok589)* mutant, where RNAi does not work in somatic cells. RNAi of *utx-1* could not extend the life span of *rrf-1(ok589)*. As a positive control, *ash-2* RNAi extended life span of *rrf-1(ok589)* worms. This experiment was done in the no-FUdR condition. Statistics are presented in Table S6. RNAi of *utx-1* could not increase life span in *rrf-1(ok589)* in +FUdR condition either (Table S5).

(H) *utx-1* RNAi increased life span in germline-defective mutant *glp-1(e2141)*. Statistics are presented in Table S5. All the experiments on N2 were done at 20°C, while experiments on *glp-1(ts)* were shifted to 25°C at the L1 stage.

See also Tables S5 and S6.

expression changes was observed in *utx-1* heterozygote *tm3118*/+ versus its balancer strain AF1 for most (including *daf-2, akt-1*, and *akt-2*) but not all IIS genes (Figure S3A). Meanwhile, the messenger RNA (mRNA) level of the *sir-2.1* gene, which affects aging by regulating *daf-16* in parallel to IIS pathway (Berdichevsky et al., 2006), was not altered by *utx-1* RNAi (Figure 5A), implying no direct regulation of *utx-1* on *sir-2.1*.

The overall transcript level of *daf-16* was also slightly reduced by *utx-1* RNAi, implying that *utx-1* may also regulate the transcript level of *daf-16*. However, the activity of *daf-16* depends on the amount of nuclear DAF-16 protein level. We therefore examined if *utx-1* RNAi could promote DAF-16 nuclear translocation. We performed *utx-1* RNAi in the TJ356 strain, which expresses a functional DAF-16::GFP fusion protein, using *daf-2* and empty vector RNAi as positive and negative controls, respectively. Worms in each RNAi experiment were classified into four categories based on DAF-16 subcellular localization: (1) nuclear, (2) mostly nuclear, (3) mostly cytoplasmic, and (4) cytoplasmic (Figure 5B). The percentage of worms in each category was then counted. In line with the phenotypes we observed, DAF-16::GFP displayed more frequent nuclear localization under *utx-1* RNAi compared to the vector RNAi, where DAF-16 had no exclusive nuclear accumulation (Figure 5B). To further confirm that DAF-16 transcription activity is increased by *utx-1* RNAi, we did qPCR to detect the expression levels of two known DAF-16 target genes, *sod-3* and *daf-15*, which are positively and negatively regulated by DAF-16, respectively (Jia et al., 2004; Oh et al., 2006). Consistent with the DAF-16 nuclear localization patterns (Figure 5B), *sod-3* increased and *daf-15* decreased in mRNA levels when *utx-1* was knocked down (Figure 5C), further

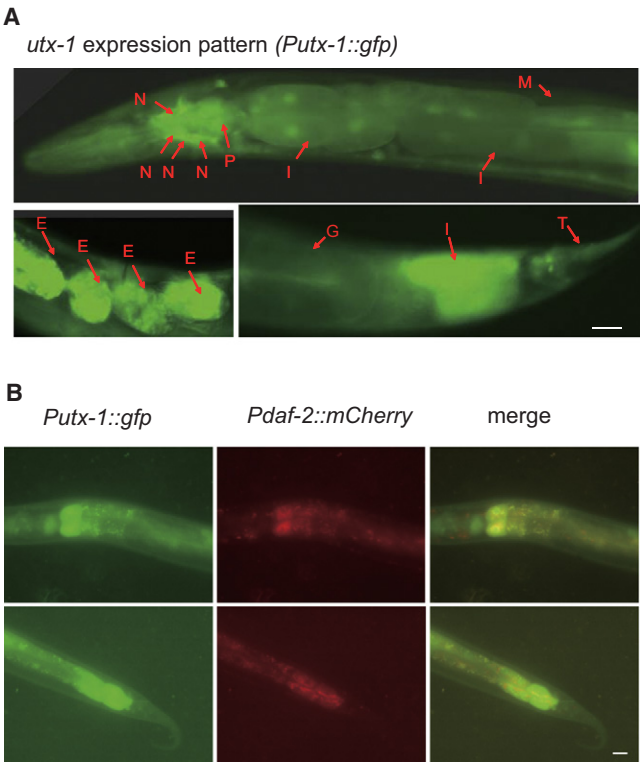

Figure 4. Ubiquitous Expression of *utx-1* At Least Partially Colocalizes with *daf-2* at Tissue Level

(A) GFP expression driven by *utx-1* promoter (*Putx-1*::gfp) displays high intensities in neurons (N), intestine (I), embryo (E), and pharynx (P), relative low intensities in muscle (M), germline (G), and tail (T). The scale bar represents 20 μm.

(B) *Putx-1*::*gfp* (green) and *Pdaf-2*::*mCherry* (red) marked *utx-1* and *daf-2* expressions are colocalized in at least some neurons and intestine. The scale bar represents 20 μm.

demonstrating *utx-1* RNAi's induction of DAF-16 activity. Therefore, the changes of IIS gene expressions and DAF-16 activity are consistent with the results of genetic epistasis analysis, and further confirmed the IIS pathway as the mediator for the life span regulation by *utx-1*.

The *utx-1* orthologs in human and zebrafish have been shown to regulate *Hox* gene expression (Agger et al., 2007; Lan et al., 2007). We therefore tested two of the six *C. elegans Hox* genes *mab-5* and *lin-39*, and found that their expression levels did not change significantly upon *utx-1* RNAi (Figure S3B). Consistently, we did not observe male tail defects associated with *mab-5* mutation or multi-vulva phenotype associated with *lin-39* (data not shown). This indicates that not all *Hox* genes are conserved *utx-1* targets in *C. elegans* as examined under partial loss of function of *utx-1*.

Changes of Expression of the IIS Genes during Aging

Next, we asked whether *utx-1*'s regulation of IIS pathway is manifested during aging by changes in their gene expression levels. Amazingly, the level of *daf-2* increased dramatically, while *age-1*, *akt-1* and *daf-16* only showed very modest increases during aging (Figure 5D). This indicates that *daf-2* might be the primary target of *utx-1* during aging for life span regulation. The increase in gene expression of *daf-2* apparently lagged behind the increase of *utx-1* during the aging time course (Figure S3C), consistent with *utx-1* increase being causal to *daf-2* increase. Further confirming this, during the time course of *utx-1* RNAi the *utx-1* mRNA level decreased early in L2, whereas the *daf-2* mRNA level decrease lagged behind *utx-1* (Figure 5E). In these experiments, we also used tubulin as another internal control, the results are essentially the same as using actin as control, and actin level did not change upon *utx-1* RNAi, at least against tubulin (Figure S3D).

UTX-1 Regulates *daf-2* Transcription by H3K27me3 Modification

As the human UTX protein can regulate the H3K27me3 level on its target genes (Lan et al., 2007), we hypothesized that *utx-1*'s transcriptional regulation of the IIS genes might be through its demethylation of the H3K27me3 marks on the IIS genes, in particular the major responder *daf-2* (Figures 5A and 5E). Using recombinant JmjC domain of *C. elegans* UTX-1, we verified that UTX-1 has demethylase activity. Incubating the wild-type JmjC domain with histones in an in vitro demethyation buffer reduced the level of H3K27me3 and H3K27me2 while increasing the level of H3K27me1 on histones (Figure 6A). The reaction was dependent on JmjC demethylase cofactors Fe^{2+}, α-ketoglutarate (α-KG), or ascorbate (Figure S4A). In contrast, UTX-1 did not demethylate H3K9me3 or H3K9me2 (Figure S4B). Also consistent with UTX-1 being an H3K27me3 demethylase in vivo, we observed an increase in the overall level of endogenous H3K27me3 in both young and aged *utx-1* RNAi worms compared with those in the same age vector-RNAi worms (Figure 6B). A similar increase in H3K27me3 can be observed in the *utx-1* heterozygous mutant *tm3118*+/− (Figure 6B). Then we performed H3K27me3 chromatin immunoprecipitation (ChIP)-qPCR to monitor the H3K27me3 levels changes in the *daf-2* gene in response to *utx-1* RNAi and between old and young worms. If UTX-1 demethylates H3K27me3 on the *daf-2* gene, downregulation of *utx-1* will cause a higher H3K27me3 level on the gene. The H3K27me3 levels along the *daf-2* locus as measured by fold enrichment over IgG normalized to input DNA decreased in the old worms compared with the young worms (Student's t test, $p < 0.01$ for all groups; Figure 6C, primers in Table S7). Additionally, the level of H3K27me3 was significantly increased by *utx-1* RNAi in the old worms (Student's t test $p < 0.05$ for all groups), whereas in young worms a small specific increase in H3K27me3 near the 5′ end of the *daf-2* gene was observed, but not in the far upstream or in an exon (Figure 6C). In line with the H3K27me3 changes, in samples processed in parallel, RNAi of *utx-1* partially repressed aging-dependent *daf-2* mRNA increase, further supporting the *utx-1* effect on *daf-2* (Figure S3C). Similar increases in H3K27me3 on the *daf-2* locus were observed by comparing *utx-1* heterozygote *tm3118*/+ with its parental AF1 strain (Figure S4C).

The age-dependent decrease in H3K27me3 and its restoration by *utx-1* RNAi in the *daf-2* locus was consistent with observable significant changes genome-wide in the same pattern in promoter regions (in particular within 1Kb upstream of transcription start sites [TSSs]), as manifested by the ChIP-seq (ChIP followed by Illumina GAII deep sequencing) profiles (Figure S4D).

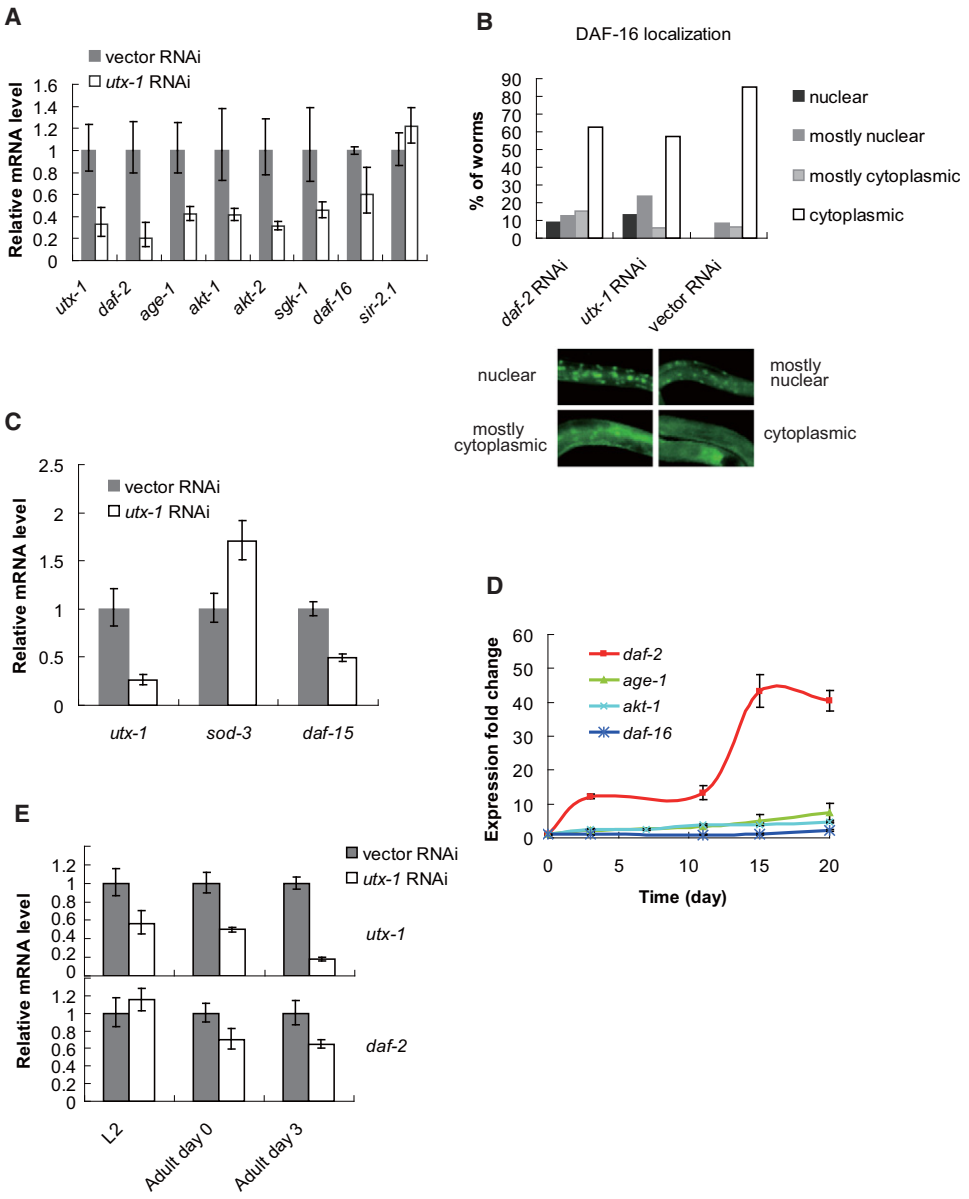

Figure 5. UTX-1 Regulates IIS Gene Expression and DAF-16 Translocation

(A) Expression level changes of IIS and *sir-2.1* upon *utx-1* RNAi. The mRNA levels of the indicated genes were measured on total RNA isolated from synchronized day 3 adult worms by qPCR. Gene expression levels were linearly scaled against the mean in the control vector RNAi worms. β-actin mRNA level was used as an internal control. Error bars represent the SEM of three repeats.

(B) RNAi of *utx-1* promoted DAF-16 translocation into nucleus. With *daf-2* RNAi as positive control, a total of 221, 162, and 209 worms were scored for DAF-16::GFP subcellular localization in DAF-16::GFP transgenic worms TJ356 upon *daf-2*, *utx-1* or vector RNAi. Scoring and counting of the subcellular distribution were done double blindly by three people. Typical DAF-16::GFP images for each category are shown in the lower panel.

(C) Expression level changes of typical targets of *daf-16*, *sod-3* and *daf-15*, known to be positively and negatively regulated by DAF-16, respectively. Expression level changes were measured at adult day 3 by qPCR with β-actin used as an internal control and were linearly scaled against the mean in the control vector RNAi worms. Error bars represent the SEM of three repeats.

(D) Changes of IIS genes expression during aging. The transcript levels were quantified by qPCR and expressed as the fold change relative to the expression levels in day 0 of adulthood. The whiskers represent the SEM among three replicates.

(E) Transcript levels of *utx-1* and *daf-2* in L2, day 0, and day 3 young adults during the time course of *utx-1* RNAi from L1 and onward in TJ356 strain. The transcript levels are scaled relative to each gene's expression level in the control vector RNAi worms at the same time point. Error bars represent the SEM of three repeats. See also Figure S3 and Table S7.

Through ChIP-seq, we also found that besides *daf-2*, *akt-1* and *akt-2* also displayed an *utx-1* RNAi dependent increase of H3K27me3 in their promoter regions in old worms, whereas *age-1, sgk-1* or *sir-2.1* did not. In addition, consistent with a lack of transcriptional change upon *utx-1* RNAi, *lin-39* and *mab-5* do not seem to be targets of *utx-1* as their H3K27me3

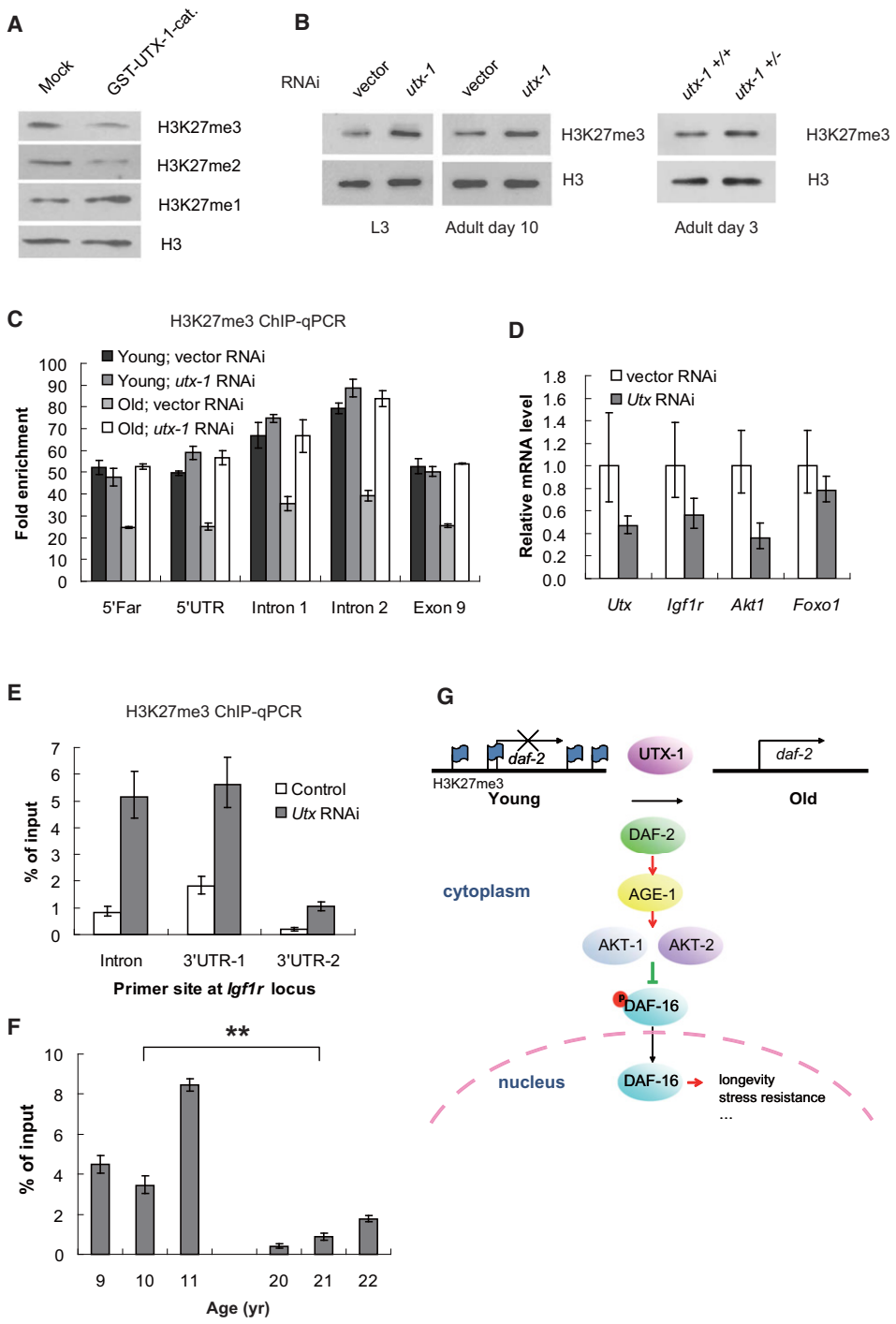

Figure 6. UTX-1 Regulates H3K27me3 Level on *daf-2/Igf1r* during Aging

(A) The GST::UTX-1 JmjC catalytic domain fusion protein catalyzed the demethylation of H3K27me2/3, but not H3K27me1 in vitro. Fusion protein (1 μg) was incubated with histone and demethylation buffer for 3 hr.

(B) Increase in cellular H3K27me3 level upon *utx-1* RNAi in both L3 and adult day 10 worms compared with control vector RNAi worms at the same stages, or in the *utx-1* heterozygous mutant *tm3118*+/− compared with its parental AF1 strain. RNAi was started from L1.

(C) H3K27me3 level determined by ChIP-qPCR on the *daf-2* gene. H3K27me3 levels were expressed as the fold enrichment over IgG normalized by the input DNA in each sample for day 3 young-adult vector and *utx-1* RNAi and day 10 old-adult vector and *utx-1* RNAi. All RNAi started from L1 stage. Error bars represent the SD. Primer sequences for qPCR are listed in Table S7.

(D) Knockdown of *Utx* in mouse 3T3-L1 cells lowers *Igf1r* transcript level. Expression levels of IIS genes quantified by qPCR in 3T3-L1 cells transfected with a construct containing shRNA compared to the same genes' expression level in empty vector-transfected control cells. β-actin mRNA level was used as an internal control. Error bars represent the SEM of three repeats.

level in the *utx-1* RNAi worms did not increase compared to that of vector RNAi (Figure S4E).

UTX-1 Regulation of IIS and Life Span Is Likely to Be Conserved in Mammals

Finally, we examined whether the UTX-1 regulation on IIS and life span uncovered in *C. elegans* is relevant to mammalian systems, as both UTX and IIS are highly conserved from invertebrates to mammals. When the endogenous *Utx* expression level in 3T3-L1 cells was downregulated by the short hairpin RNA (shRNA) specifically targeting the *Utx* gene, a remarkable decrease of *Igf1r* expression level was detected by qPCR (Figure 6D, primers in Table S7). Similar decreases were also observed for IIS downstream genes exactly as we observed for the *C. elegans* IIS genes (Figure 5A). These results indicate that *utx-1* regulation of the IIS pathway is conserved between *C. elegans* and mouse.

In H3K27me3 ChIP-qPCR experiments, as expected, H3K27me3 modification levels along *Igf1r* displayed a 3 to 7 fold increase after *Utx* RNAi as detected by three different primer sets (Figure 6E, primers in Table S7).

To examine whether UTX demethylase activity is also relevant to the mammalian aging process, we examined the level of H3K27me3 modification on *IGF1R* during aging by ChIP-qPCR with macaque muscle samples. Based on the syntenic regions corresponding to the most sensitive primer set we found for mouse *Igf1r* (Figure 6E), we indeed found a significant age-dependent decrease of H3K27me3 relative to the level in input DNA in each sample (Figure 6F, primers in Table S7; Student's t test, $p = 0.000153$). A similar age-associated decrease was observed by ChIP-seq on the *IGF1R* gene in macaque brains (J.-D.J.H., unpublished data, and Figure S4F).

DISCUSSION

Our data suggest a model (Figure 6G) in which UTX-1 is a transcription regulator of the IIS pathway through epigenetically regulating its gene expression levels. In this model, UTX-1/UTX functions as a demethylase that is capable of removing the gene expression repressive mark H3K27me3 on the IIS pathway genes, in particular the *daf-2*/*Igf1r* gene. Its increase at midlife of adult life span activates the IIS, ultimately reducing the FOXO/DAF-16 protein level in the nucleus, which results in decreased cellular maintenance functions and an aging-related decline in cellular functions. Reduction of the UTX-1 activity, currently by RNAi and mutagenesis and hopefully in the future by small molecular drugs, can reverse this adverse effect of age-dependent increase in UTX activity, thereby reestablishing a more "naïve" or "younger" epigenetic status of the IIS pathway which eventually delays (or might also reverse) the aging process. This model is supported by five major findings: (1) The expression of human UTX and its worm homolog increased in the human brain and *C. elegans* during the aging process. Its sharp midlife increase in *C. elegans* precedes the dramatic elevation of *daf-2* expression and the increase in mortality. (2) *utx-1* RNAi significantly extended *C. elegans* life span in a manner dependent on the key players of the IIS pathway, such as *daf-2*, *akt-1*, *akt-2* and *daf-16* activities. (3) *utx-1* regulates the gene expression of the IIS pathway, in particular DAF-16 nuclear translocation. (4) UTX-1 protein regulates *daf-2*/*Igf1r* expression by acting as a H3K27me3 demethylase. (5) In line with the increased *daf-2* gene expression during aging, H3K27me3 on the *daf-2*/*Igf1r* decreased dramatically in old animals (both worms and monkeys).

RNAi of *utx-1* during embryonic stage results in embryonic lethality, thus *utx-1* is required for early development as is the IIS pathway. We did not observe any obvious postembryonic phenotypes other than life span extension, as found previously (Agger et al., 2007). So far, only one screen attempted to tackle the 2700 essential genes postdevelopmentally (Curran and Ruvkun, 2007). It is not known whether *utx-1* was included in the 2700 gene list or lost during the screen. Modeled after Curran et al.'s study, we carried out *utx-1* RNAi at the postembryonic developmental stage.

Interestingly, the H3K27me3 decrease with age can be also observed at genome-wide level in promoter regions, and can be restored by *utx-1* RNAi (Figure S4D), indicating a global downregulation of H3K27me3 at many gene loci might result from the increased *utx-1* expression in old worms. Therefore, *utx-1* might not specifically target IIS genes, but instead, IIS genes serve as sensors for the global epigenetic status change and tune downstream cell growth and stress resistance functions accordingly.

Given the tight association of aging with nearly all complex human diseases, delaying the aging process might also delay the onset of these complex diseases. Our findings revealed an epigenetic regulation on aging, which to our knowledge is the first report of a histone methylation-modifying gene participating in normal aging regulation in adult somatic tissue. Previously, the ASH-2 complex, which trimethylates H3K4, was identified as an aging regulator that acted in germline (Greer et al., 2010). Such an indirect life span regulation on the soma has not been shown to be conserved in mammals. The only somatic tissue epigenetic regulator of aging discovered is the Sir2 gene. Different from the well-known Sir2 histone deacetylase (Dang et al., 2009;

(E) H3K27me3 modification level determined by ChIP-qPCR in 3T3-L1 cells transfected with empty vector or constructs containing shRNA. The qPCR signal is expressed as percentage of the qPCR signal on total input DNA. Error bars represent the SEM of three repeats. The sequences of the primers are presented in Table S7.

(F) H3K27me3 modification levels in the second intron of the *IGF1R* gene in three young (9, 10, and 11 year old) and three old (20, 21, and 22 year old) male macaque muscle samples as determined by ChIP-qPCR. Primers used correspond to the "intron" site listed in Table S7. The qPCR signal is expressed as the percentage over the corresponding input DNA from each sample. Error bars represent the SEM of three repeats. The significance of the difference between young and old groups was determined by the Student's t test. ** indicates $p < 0.001$.

(G) A model for histone demethylase *utx-1* regulating life span by targeting IGF-1 pathway. UTX-1 as an H3K27me2/3 demethylase increases during aging, activating the insulin-like signal receptor DAF-2 transcription by decreasing the H3K27me3 silencing mark on the gene and also its downstream genes, which ultimately prevents DAF-16 translocation from cytoplasm to nucleus. This in turn leads to decreased longevity and stress resistance of the animals. RNAi against *utx-1* can block such a negative effect of *utx-1* on longevity by resetting a "younger" epigenetic status of the IIS pathway.

See also Figure S4 and Table S7.

Guarente and Picard, 2005; Oberdoerffer et al., 2008) that plays an important role in genome stability, UTX-1, similar to its target IIS pathway, is an important development regulator. Aging can be seen as a special, late developmental stage that, unlike early development, is not directly under reproductive or evolutionary selection pressure (Kirkwood, 2005). During early development and aging, the genomes of individual cells remain largely the same. Changes in the transcriptome can be memorized by the cells or even passed on to the next generation of cells through epigenetic modifications on the genomes. As erasing these marks set up in the developmental stage can help reverse the differentiated states to undifferentiated or even pluripotent stem cell states (Boyer et al., 2006; Huangfu et al., 2008; Yamanaka, 2009), it is tempting to speculate that reestablishing the epigenetic marks erased by the aging process might also help reverse the aging process.

EXPERIMENTAL PROCEDURES

C. elegans Strains

The strain *tm3118* was a gift from Shohei Mitani. All other *C. elegans* strains were obtained from the *Caenorhabditis* Genetics Center: CB1370, *daf-2(e1370)* III; CF1038, *daf-16(mu86)* I; RB759, *akt-1(ok525)* V; VC204, *akt-2(ok393)* X; VC345, *sgk-1(ok538)* X; RB798, *rrf-1(ok589)* I; CF1903, *glp-1(e2141)* III; AF1, *+/szT1[lon-2(e678)]* I *dpy-8(e1321) unc-3(e151)/szT1* X; VC2862, *+/szT1[lon-2(e678)]* I; *utx-1(ok3553)/szT1 X*; TJ356, *zls356* IV. Nematodes were cultured via standard methods (Brenner, 1974). *utx-1 +/−*, *+/szT1 [lon-2(e678)]* I *utx-1(tm3118)/szT1* was obtained by crossing tm3118 with AF1.

Constructs for Worms

Constructs were done by standard molecular techniques. Detailed procedures and primers are described in the Supplemental Experimental Procedures.

Life Span Assay

Life span assay was done as described previously (Xue et al., 2007). In brief, synchronized eggs grown to young adult stage were distributed to RNAi or non-RNAi plates containing 20 μg/ml FUdR to prevent progeny growth. For RNAi, bacteria clones were selected from Ahringer's RNAi feeding bacteria library (Kamath et al., 2003), and dsRNA expression was induced by 1 mM IPTG. The same HT115 bacteria carrying the empty L4440 construct were used as controls in all experiments. The worms were cultured at 20°C unless specified and transferred to fresh RNAi plates every 4 days to ensure continued efficacy of RNAi knockdown. Worms that crawled off were excluded from the experiments. The number of dead worms was counted every other day. All experiments were independently performed at least twice. The p value was calculated by log-rank test on the Kaplan-Meier curves.

Stress Tolerance Assays

Synchronized L1 worms were grown on nematode growth medium plates with or without RNAi. On day 3 of adult stage, for heat stress, the plates were transferred to 35°C incubator, and the number of dead worms was counted every 3 hr. For UV-resistant stress, plates were exposed to 1200 J/m^2 UV and then recovered at standard culture condition, and mortality was counted every day. For paraquat stress, worms were transferred to 100 mM paraquat (Sigma) in S-basal medium, and mortality was counted every other hour (Dillin et al., 2002).

Expression and Purification of GST-JmjC Domain of *C. elegans* UTX-1

To clone JmjC domain of UTX-1, primers cgcGGATCCGAGTATCAATCGG AATCGTTCAAGCACAC and cgcGTCGACCTAGGCAGTGAAACTCATCTTAT TGTTGTTAGCTG with BamHI and SalI digestion sites were used for PCR the sequence encoding 802–1168 amino acid of UTX-1 from N2 worm complementary DNA (cDNA). The PCR product was inserted in to pGEX-4T-1 plasmid with an N-terminal GST tag. GST-JmjC domain of UTX-1 was expressed in Rosetta *E. coli,* and the protein was purified according to a standard protocol.

Demethylation Assay

Bulk calf thymus type II-A histone proteins (Sigma #H9250) were incubated with the purified fusion protein of GST-JmjC domain of UTX-1 in demethylation buffer [20 mM Tris-HCl pH 7.5, 150 mM NaCl, 50 μM $(NH_4)_2Fe(SO_4)_2$+6(H_2O), 1 mM α-ketoglutarate, and 2 mM ascorbic acid] for 3 hr at 37°C. A total of 1 μg fusion protein and 1 μg bulk histones were included in 20 μl reaction. The reaction was stopped with SDS loading buffer, and western blot analysis was performed.

H3K27me3 Western Blot from Worm Sample

Worms were grown synchronously to appropriate stages and washed with M9 buffer, boiled in loading buffer without bromophenol blue before measuring total protein concentration. Five micrograms of total protein was loaded in a 15% SDS-PAGE. Anti-H3K27me3 1:3000, anti-H3 1:2000 antibodies (abcam) were used for blotting.

Gene Expression Level Detected by Real-Time Quantitative PCR

Total RNA was isolated from worms with TRIzol reagent (Invitrogen). Reverse transcriptase (TOYOBO) was used for oligo (dT) primed first-strand cDNA synthesis. The qPCR analysis was carried out on an Mx3000P (Stratagene) with EvaGreen dye (Biotium). The ΔΔCt method was used to quantify the amount of mRNA level relative to that of β-actin (Livak and Schmittgen, 2001). The oligonucleotides used for PCR are listed in Table S7.

DAF-16 Translocation Detection

Larva stage of TJ356 (*zls356* IV) worms were cultured under standard RNAi condition. One day later, the GFP immunofluorescence was observed under microscope. Worms were divided into four categories according to the GFP distribution: those with GFP in cytoplasm, most in cytoplasm, most in nucleus, and in nucleus, as previously described (Padmanabhan et al., 2009). The number of worms in each category was then counted for each RNAi group, and finally the percentage of each category was scored by three experimenters independently not knowing the labels of the samples.

ChIP-qPCR, ChIP-Seq Data Generation and Analysis

Worms used for ChIP were cultured on plates with 10× condensed food; young and old samples were collected on adult day 3 and 10, when nearly all worms were still alive. ChIP in *C. elegans* was performed after crosslinking in 1% formaldehyde for 20 min as described (Mukhopadhyay et al., 2008) with a purified antibody. For additional information and ChIP-seq analysis and ChIP of other samples, see the Supplemental Experimental Procedures.

Construct of shRNA against the Mouse *Utx* Gene

The shRNA construct against *Utx* targeting GCCUAGCAAUUCAGUAACA was used to insert into plasmid pll3.7. The plasmids were transfected into 3T3-L1 cells with the VigoFect transfection reagent, and cells were collected 48 hr after transfection.

ACCESSION NUMBERS

Our *C. elegans* H3K27me3 ChIP-seq data have been deposited in the GEO database under accession number GSE29896.

SUPPLEMENTAL INFORMATION

Supplemental Information includes Supplemental Experimental Procedures, four figures, and seven tables and can be found with this article online at doi:10.1016/j.cmet.2011.07.001.

ACKNOWLEDGMENTS

We thank Shohei Mitani for providing the *tm3118* deletion allele and Michael Levine, Nicholas Baker, and Dangsheng Li for invaluable suggestions. We are indebted to Teng Fei, Yeguang Chen, Chonglin Yang, Mei Ding, and Zhukuan Cheng for sharing equipment. This work was supported by grants

from the China Natural National Science Foundation (NSFC; grant numbers 30890033 and 91019019), the Chinese Ministry of Science and Technology (grant number 2011CB504206), and the Chinese Academy of Sciences (CAS; grant numbers KSCX2-EW-R-02 and KSCX2-EW-J-15), and stem cell leading project XDA01010303 to J.D.J.H. C.D.G. is supported by the CAS and a NSFC young foreign investigator fellowship.

Received: December 20, 2010
Revised: April 7, 2011
Accepted: June 13, 2011
Published: August 2, 2011

REFERENCES

Agger, K., Cloos, P.A., Christensen, J., Pasini, D., Rose, S., Rappsilber, J., Issaeva, I., Canaani, E., Salcini, A.E., and Helin, K. (2007). UTX and JMJD3 are histone H3K27 demethylases involved in HOX gene regulation and development. Nature *449*, 731–734.

Antebi, A. (2007). Genetics of aging in Caenorhabditis elegans. PLoS Genet. *3*, 1565–1571.

Arantes-Oliveira, N., Berman, J.R., and Kenyon, C. (2003). Healthy animals with extreme longevity. Science *302*, 611.

Berdichevsky, A., Viswanathan, M., Horvitz, H.R., and Guarente, L. (2006). C. elegans SIR-2.1 interacts with 14-3-3 proteins to activate DAF-16 and extend life span. Cell *125*, 1165–1177.

Berger, S.L. (2007). The complex language of chromatin regulation during transcription. Nature *447*, 407–412.

Boyer, L.A., Plath, K., Zeitlinger, J., Brambrink, T., Medeiros, L.A., Lee, T.I., Levine, S.S., Wernig, M., Tajonar, A., Ray, M.K., et al. (2006). Polycomb complexes repress developmental regulators in murine embryonic stem cells. Nature *441*, 349–353.

Brenner, S. (1974). The genetics of Caenorhabditis elegans. Genetics *77*, 71–94.

Brosch, G., Loidl, P., and Graessle, S. (2008). Histone modifications and chromatin dynamics: a focus on filamentous fungi. FEMS Microbiol. Rev. *32*, 409–439.

Campisi, J. (2005). Senescent cells, tumor suppression, and organismal aging: good citizens, bad neighbors. Cell *120*, 513–522.

Chien, K.R., and Karsenty, G. (2005). Longevity and lineages: toward the integrative biology of degenerative diseases in heart, muscle, and bone. Cell *120*, 533–544.

Curran, S.P., and Ruvkun, G. (2007). Lifespan regulation by evolutionarily conserved genes essential for viability. PLoS Genet. *3*, e56.

Dang, W., Steffen, K.K., Perry, R., Dorsey, J.A., Johnson, F.B., Shilatifard, A., Kaeberlein, M., Kennedy, B.K., and Berger, S.L. (2009). Histone H4 lysine 16 acetylation regulates cellular lifespan. Nature *459*, 802–807.

De Santa, F., Totaro, M.G., Prosperini, E., Notarbartolo, S., Testa, G., and Natoli, G. (2007). The histone H3 lysine-27 demethylase Jmjd3 links inflammation to inhibition of polycomb-mediated gene silencing. Cell *130*, 1083–1094.

Dillin, A., Crawford, D.K., and Kenyon, C. (2002). Timing requirements for insulin/IGF-1 signaling in C. elegans. Science *298*, 830–834.

Finkel, T., and Holbrook, N.J. (2000). Oxidants, oxidative stress and the biology of ageing. Nature *408*, 239–247.

Greer, E.L., Maures, T.J., Hauswirth, A.G., Green, E.M., Leeman, D.S., Maro, G.S., Han, S., Banko, M.R., Gozani, O., and Brunet, A. (2010). Members of the H3K4 trimethylation complex regulate lifespan in a germline-dependent manner in C. elegans. Nature *466*, 383–387.

Guarente, L., and Picard, F. (2005). Calorie restriction—the SIR2 connection. Cell *120*, 473–482.

Harman, D. (2006). Alzheimer's disease pathogenesis: role of aging. Ann. N Y Acad. Sci. *1067*, 454–460.

Hertweck, M., Göbel, C., and Baumeister, R. (2004). C. elegans SGK-1 is the critical component in the Akt/PKB kinase complex to control stress response and life span. Dev. Cell *6*, 577–588.

Hong, S., Cho, Y.W., Yu, L.R., Yu, H., Veenstra, T.D., and Ge, K. (2007). Identification of JmjC domain-containing UTX and JMJD3 as histone H3 lysine 27 demethylases. Proc. Natl. Acad. Sci. USA *104*, 18439–18444.

Hsu, A.L., Murphy, C.T., and Kenyon, C. (2003). Regulation of aging and age-related disease by DAF-16 and heat-shock factor. Science *300*, 1142–1145.

Huangfu, D., Osafune, K., Maehr, R., Guo, W., Eijkelenboom, A., Chen, S., Muhlestein, W., and Melton, D.A. (2008). Induction of pluripotent stem cells from primary human fibroblasts with only Oct4 and Sox2. Nat. Biotechnol. *26*, 1269–1275.

Jia, K., Chen, D., and Riddle, D.L. (2004). The TOR pathway interacts with the insulin signaling pathway to regulate C. elegans larval development, metabolism and life span. Development *131*, 3897–3906.

Jiang, Y., Langley, B., Lubin, F.D., Renthal, W., Wood, M.A., Yasui, D.H., Kumar, A., Nestler, E.J., Akbarian, S., and Beckel-Mitchener, A.C. (2008). Epigenetics in the nervous system. J. Neurosci. *28*, 11753–11759.

Kamath, R.S., Fraser, A.G., Dong, Y., Poulin, G., Durbin, R., Gotta, M., Kanapin, A., Le Bot, N., Moreno, S., Sohrmann, M., et al. (2003). Systematic functional analysis of the Caenorhabditis elegans genome using RNAi. Nature *421*, 231–237.

Kenyon, C. (2005). The plasticity of aging: insights from long-lived mutants. Cell *120*, 449–460.

Kimura, K.D., Tissenbaum, H.A., Liu, Y., and Ruvkun, G. (1997). daf-2, an insulin receptor-like gene that regulates longevity and diapause in Caenorhabditis elegans. Science *277*, 942–946.

Kirkwood, T.B. (2005). Understanding the odd science of aging. Cell *120*, 437–447.

Klose, R.J., and Zhang, Y. (2007). Regulation of histone methylation by demethylimination and demethylation. Nat. Rev. Mol. Cell Biol. *8*, 307–318.

Lamitina, S.T., and Strange, K. (2005). Transcriptional targets of DAF-16 insulin signaling pathway protect C. elegans from extreme hypertonic stress. Am. J. Physiol. Cell Physiol. *288*, C467–C474.

Lan, F., Bayliss, P.E., Rinn, J.L., Whetstine, J.R., Wang, J.K., Chen, S., Iwase, S., Alpatov, R., Issaeva, I., Canaani, E., et al. (2007). A histone H3 lysine 27 demethylase regulates animal posterior development. Nature *449*, 689–694.

Lee, S.S., Kennedy, S., Tolonen, A.C., and Ruvkun, G. (2003). DAF-16 target genes that control *C. elegans* life-span and metabolism. Science *300*, 644–647.

Lee, M.G., Villa, R., Trojer, P., Norman, J., Yan, K.P., Reinberg, D., Di Croce, L., and Shiekhattar, R. (2007). Demethylation of H3K27 regulates polycomb recruitment and H2A ubiquitination. Science *318*, 447–450.

Li, B., Carey, M., and Workman, J.L. (2007). The role of chromatin during transcription. Cell *128*, 707–719.

Libina, N., Berman, J.R., and Kenyon, C. (2003). Tissue-specific activities of C. elegans DAF-16 in the regulation of lifespan. Cell *115*, 489–502.

Lin, K., Dorman, J.B., Rodan, A., and Kenyon, C. (1997). daf-16: An HNF-3/forkhead family member that can function to double the life-span of Caenorhabditis elegans. Science *278*, 1319–1322.

Lithgow, G.J., White, T.M., Melov, S., and Johnson, T.E. (1995). Thermotolerance and extended life-span conferred by single-gene mutations and induced by thermal stress. Proc. Natl. Acad. Sci. USA *92*, 7540–7544.

Livak, K.J., and Schmittgen, T.D. (2001). Analysis of relative gene expression data using real-time quantitative PCR and the 2(-Delta Delta C(T)) Method. Methods *25*, 402–408.

Longo, V.D., and Kennedy, B.K. (2006). Sirtuins in aging and age-related disease. Cell *126*, 257–268.

Lu, T., Pan, Y., Kao, S.Y., Li, C., Kohane, I., Chan, J., and Yankner, B.A. (2004). Gene regulation and DNA damage in the ageing human brain. Nature *429*, 883–891.

Martin, C., and Zhang, Y. (2005). The diverse functions of histone lysine methylation. Nat. Rev. Mol. Cell Biol. *6*, 838–849.

McKay, S.J., Johnsen, R., Khattra, J., Asano, J., Baillie, D.L., Chan, S., Dube, N., Fang, L., Goszczynski, B., Ha, E., et al. (2003). Gene expression profiling

of cells, tissues, and developmental stages of the nematode C. elegans. Cold Spring Harb. Symp. Quant. Biol. *68*, 159–169.

Morris, J.Z., Tissenbaum, H.A., and Ruvkun, G. (1996). A phosphatidylinositol-3-OH kinase family member regulating longevity and diapause in Caenorhabditis elegans. Nature *382*, 536–539.

Mukhopadhyay, A., Deplancke, B., Walhout, A.J., and Tissenbaum, H.A. (2008). Chromatin immunoprecipitation (ChIP) coupled to detection by quantitative real-time PCR to study transcription factor binding to DNA in Caenorhabditis elegans. Nat. Protoc. *3*, 698–709.

Murakami, S., and Johnson, T.E. (1996). A genetic pathway conferring life extension and resistance to UV stress in Caenorhabditis elegans. Genetics *143*, 1207–1218.

Murphy, C.T., McCarroll, S.A., Bargmann, C.I., Fraser, A., Kamath, R.S., Ahringer, J., Li, H., and Kenyon, C. (2003). Genes that act downstream of DAF-16 to influence the lifespan of Caenorhabditis elegans. Nature *424*, 277–283.

Oberdoerffer, P., Michan, S., McVay, M., Mostoslavsky, R., Vann, J., Park, S.K., Hartlerode, A., Stegmuller, J., Hafner, A., Loerch, P., et al. (2008). SIRT1 redistribution on chromatin promotes genomic stability but alters gene expression during aging. Cell *135*, 907–918.

Ogg, S., Paradis, S., Gottlieb, S., Patterson, G.I., Lee, L., Tissenbaum, H.A., and Ruvkun, G. (1997). The Fork head transcription factor DAF-16 transduces insulin-like metabolic and longevity signals in C. elegans. Nature *389*, 994–999.

Oh, S.W., Mukhopadhyay, A., Dixit, B.L., Raha, T., Green, M.R., and Tissenbaum, H.A. (2006). Identification of direct DAF-16 targets controlling longevity, metabolism and diapause by chromatin immunoprecipitation. Nat. Genet. *38*, 251–257.

Padmanabhan, S., Mukhopadhyay, A., Narasimhan, S.D., Tesz, G., Czech, M.P., and Tissenbaum, H.A. (2009). A PP2A regulatory subunit regulates C. elegans insulin/IGF-1 signaling by modulating AKT-1 phosphorylation. Cell *136*, 939–951.

Paradis, S., and Ruvkun, G. (1998). Caenorhabditis elegans Akt/PKB transduces insulin receptor-like signals from AGE-1 PI3 kinase to the DAF-16 transcription factor. Genes Dev. *12*, 2488–2498.

Paradis, S., Ailion, M., Toker, A., Thomas, J.H., and Ruvkun, G. (1999). A PDK1 homolog is necessary and sufficient to transduce AGE-1 PI3 kinase signals that regulate diapause in Caenorhabditis elegans. Genes Dev. *13*, 1438–1452.

Shi, Y. (2007). Histone lysine demethylases: emerging roles in development, physiology and disease. Nat. Rev. Genet. *8*, 829–833.

Shumaker, D.K., Dechat, T., Kohlmaier, A., Adam, S.A., Bozovsky, M.R., Erdos, M.R., Eriksson, M., Goldman, A.E., Khuon, S., Collins, F.S., et al. (2006). Mutant nuclear lamin A leads to progressive alterations of epigenetic control in premature aging. Proc. Natl. Acad. Sci. USA *103*, 8703–8708.

Swigut, T., and Wysocka, J. (2007). H3K27 demethylases, at long last. Cell *131*, 29–32.

Wang, J.K., Tsai, M.C., Poulin, G., Adler, A.S., Chen, S., Liu, H., Shi, Y., and Chang, H.Y. (2010). The histone demethylase UTX enables RB-dependent cell fate control. Genes Dev. *24*, 327–332.

Weishaupt, H., Sigvardsson, M., and Attema, J.L. (2010). Epigenetic chromatin states uniquely define the developmental plasticity of murine hematopoietic stem cells. Blood *115*, 247–256.

Wu, S.C., and Zhang, Y. (2009). Minireview: role of protein methylation and demethylation in nuclear hormone signaling. Mol. Endocrinol. *23*, 1323–1334.

Xue, H., Xian, B., Dong, D., Xia, K., Zhu, S., Zhang, Z., Hou, L., Zhang, Q., Zhang, Y., and Han, J.D. (2007). A modular network model of aging. Mol. Syst. Biol. *3*, 147.

Yamanaka, S. (2009). Elite and stochastic models for induced pluripotent stem cell generation. Nature *460*, 49–52.

Yu, H., Zhu, S., Zhou, B., Xue, H., and Han, J.D. (2008). Inferring causal relationships among different histone modifications and gene expression. Genome Res. *18*, 1314–1324.